Articles

Circular Differential Scattering and Circular Differential Absorption of DNA–Protein Condensates and of Dyes Bound to DNA–Protein Condensates†

Cynthia L. Phillips,‡ William E. Mickols,*,§ Marcos F. Maestre,‡ and Ignacio Tinoco, Jr.§

Division of Biology and Medicine, Lawrence Berkeley Laboratory, and Department of Chemistry and Laboratory of Chemical Biodynamics, University of California, Berkeley, California 94720

Received July 9, 1986

ABSTRACT: DNA–protein condensates that give positive and negative ψ-type circular dichroism (CD) spectra (ψ condensates) bind intercalative and nonintercalative dyes. CD depends both on circular differential scattering and on circular differential absorption; scattering-corrected CD measurements are approximations to circular differential absorption. The circular differential scattering and scattering-corrected CD patterns observed in the DNA absorption band of ψ condensates are mimicked in the induced CD band of intercalators bound to ψ condensates. The induced scattering-corrected CD and circular differential scattering patterns of the groove-binding dye Hoechst 33342 bound to ψ condensates are the inverse of the patterns seen with intercalative dyes, whereas the groove-binding dye manganese(III) *meso*-tetrakis(4-*N*-methylpyridyl)porphine [Mn^{III}TMpyP-4] shows no significant induced CD patterns. The large circular differential scattering and scattering-corrected CD bands are interpreted as resulting from long-range chiral packing, rather than near-neighbor short-range interactions. Dyes intercalated into the DNA of the ψ condensates have the same type of long-range chiral packing as the DNA bases. Therefore, the ψ-type CD spectra seen in the UV spectra originating from the long-range packing of the DNA bases are also observed in the visible spectra when dyes are intercalated in the DNA of the ψ condensates. Our interpretation comes from the observation that the induced circular differential scattering and circular differential absorption of the dye bound to the ψ condensates depend only upon the sign of the circular differential absorption and the pattern of the circular differential scattering of the ψ condensates without bound dye. The variation in the induced CD patterns of the two groove-binding dyes is attributed to small but significant binding angle changes. Conventional CD signals from dyes bound to uncondensed DNA vary for different dyes and show no particular trends. Condensation of calf thymus DNA with poly(lysine-alanine) and polylysine produced positive and negative ψ-type CD spectra, respectively. Five intercalative dyes and two dyes that bind in the minor groove of DNA were used in this investigation: ethidium, proflavin, H_2TMpyP-4, Cu^{II}TMpyP-4, and Ni^{II}TMpyP-4 (intercalative dyes); Mn^{III}TMpyP-4 and Hoechst 33342 (bind in the DNA minor groove).

Condensed forms of DNA are found in many kinds of life from viruses to cysts of bacteria to eukaryotes. Two of the most obvious places where condensed DNA in higher eukaryotes is observed are in chromosomes and in sperm (Lefevre, 1976; Lindsley, 1980). Several proposed model systems have been studied by various physical chemistry methods. One spectroscopically well-defined form of condensed DNA is the ψ form (Lerman, 1973).

ψ condensates are characterized by very large circular dichroism (CD) extinction coefficients. Light scattering is an important part of the total absorption spectrum of ψ condensates, and it is also an important contribution to the CD. CD depends both on circular differential absorption and on circular differential scattering. Several experimental methods have been developed to correct for circular differential scattering in CD spectra (Reich et al., 1980; Maestre, 1984) in order to see primarily circular differential absorption. The scattering-corrected CD spectra of ψ DNA condensates do not look like classic uncondensed DNA CD spectra. The magnitude and shape of the CD spectra (composed of both circular differential absorption and circular differential scattering) and the magnitude and shape of the circular differential scattering can be independent of each other. They are often dependent on the preparation conditions. The conditions to produce ψ-type spectra include nonaqueous solvents (Gray, 1978), high salt concentration, the presence of polymers (Jordan, 1972; Carroll, 1970), and gelation into fibers (Tunis-Schneider & Maestre, 1970). Small changes in preparation cause large changes in the spectra. Differences in CD extinction coefficient are found from researcher to researcher and from preparation to preparation. These variable results do not imply poor technique but that the range of effects obtainable within a small range of experimental conditions is large. These results also imply that a ψ preparation is a continuum of closely related structures.

X-ray diffraction of fibers pulled from solutions of ψ DNA condensates show the B conformation for the secondary structure of DNA (Maniatis, 1974). This has lead to the proposal that the anomalous CD spectra of DNA condensates are due to liquid-crystal-like packing of the DNA (Kielland & Williams, 1976; Reich et al., 1980; Maestre & Reich, 1980). Evdokimov (1983) has shown that the CD spectrum of the DNA binding drug daunomycin is altered when bound to ψ condensates. High concentrations of daunomycin invert the ψ CD spectra of both the DNA and the dye. Low concentrations of daunomycin do not invert the DNA CD, but at all

† This research was supported by grants from the National Institutes of Health (GM 10840 and RR 01613) and the U.S. Department of Energy (DE-FG03-82ER60406) to I.T. and the National Institutes of Health (AI 08427) to M.F.M.

‡ Division of Biology and Medicine, Lawrence Berkeley Laboratory.
§ Department of Chemistry and Laboratory of Chemical Biodynamics.

0006-2960/86/0425-7803$01.50/0

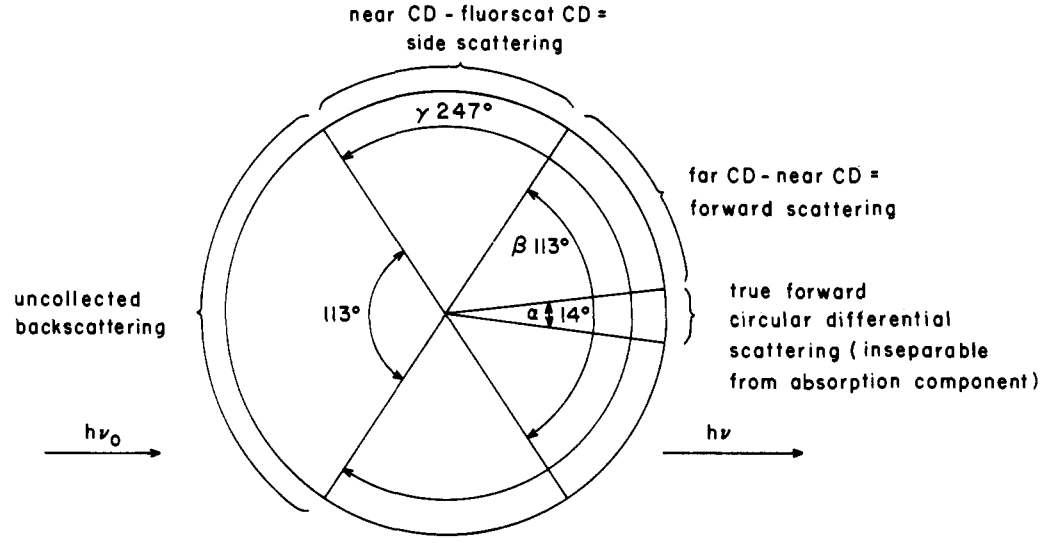

FIGURE 1: Acceptance angles of CD experiments. The photomultiplier acceptance angles for the three types of CD measurements made are $\alpha = 14°$ = far-CD acceptance angle (photomultiplier far from cuvette), $\beta = 113°$ = near-CD acceptance angle (photomultiplier close to cuvette, partially corrects for scattering), and $\gamma = 247°$ = fluorscat CD acceptance angle (a fluorescent solution surrounds most of the sample and corrects for most of the scattering, approximating circular differential absorption). The braces around the circle show the angles involved in the of circular differential scattering difference spectra reported: far-CD minus near-CD scattering (forward scattering) and near-CD minus fluorscat CD scattering (side scattering).

concentrations the dye mimics the DNA ψ-type spectra. Moreover, the induced CD of aclacinomycin A mimics that of the ψ-type DNA spectra. However, Evdokimov also reports on several other strong intercalators that do not have ψ-type CD spectra in the dye bands.

We have studied ψ condensates prepared by condensing DNA with either polylysine or poly(lysine-alanine) to produce large ψ-type UV CD spectra. Dyes with no intrinsic CD, and no CD induced by binding to polylysine or poly(lysine-alanine), were bound to the ψ condensates and found to take on the ψ spectral characteristics of the DNA. Scattering-corrected CD spectra were generated to approximate circular differential absorption spectra by using fluorscat cuvettes (Maestre, 1984) or by altering the acceptance angles of the detector (see Experimental Procedures). The intercalative dyes used (ethidium, proflavin, H_2TMpyP-4, Cu^{II}TMpyP-4, and Ni^{II}TMpyP-4) have different CD spectra when bound to uncondensed DNA, but all have a similar CD spectra when bound to ψ DNA condensates. The circular differential scattering and scattering-corrected CD spectra of the intercalative dyes bound to ψ condensates mimic the circular differential scattering and scattering-corrected CD spectra in the DNA bands of the condensed DNA with and without dye bound to it. Two dyes that do not intercalate in DNA do not show the mimicking CD patterns when bound to DNA. The groove-binding dye Hoechst 33342 has inverted ψ-type circular differential scattering and absorption spectra, and the groove-binding dye Mn^{III}TMpyP-4 (Pasternack, 1983a) has little or no ψ-type CD spectra. Our measurements show that it is not the short-range structure (nearest-neighbor or other near-neighbor interactions) that controls the CD spectra of the dyes in ψ condensates, but it is the long-range chiral order and the relative orientation of the transition dipoles to the those of the DNA. For this reason, a small amount of condensed DNA with ψ-type characteristics in a larger background of non-ψ DNA can be detected by using several dyes and by checking to see that the visible circular differential scattering and absorption spectra of the bound dyes are similar.

Further results of these studies show the ψ-type CD spectra are due to the condensed nucleic acid, not the peptide chromophores. Thus, condensed ψ DNA could be detected in a complex cellular environment from the ψ-type CD spectra in the visible region that is induced by bound dyes. By the appropriate choice of dyes, this type of induced CD will allow separation of a DNA signal from the RNA and protein contributions. This is important in such complex systems as the ψ-condensed DNA seen in mitotic Chinese hamster ovary cells (Maestre et al., 1985).

Experimental Procedures

Techniques for Measuring Total Absorption, Circular Differential Scattering, and Circular Differential Absorption Components. All CD measurements were made on a computer-interfaced Cary 60 spectropolarimeter equipped with a Cary 6001 accessory and a photomultiplier on a sliding mount. Scattering-corrected CD measurements were taken to approximate true circular differential absorption. Fluorscat cuvettes (Maestre, 1984) were used for measurements on nonfluorescent solutions and near CD measurements were made on both fluorescent (containing the dye ethidium, proflavin, or Hoechst 33342) and nonfluorescent solutions. A fluorscat cuvette is a normal cylindrical cuvette surrounded by a fluorescent solution (fluorescein), which absorbs and then fluoresces scattered light so that the closely mounted photomultiplier collects that scattered light, changing the effective average acceptance angle of the photomultiplier from 14° (conventional far CD) to about 250° (Figure 1). The external compartment of the fluorscat cuvette was filled with fluorescein at an optical density of greater than 2.0 for CD measurements throughout the near-UV and visible spectrum. Near-CD measurements were made in a normal cylindrical cuvette by sliding the photomultiplier as close as possible to the cuvette to increase the average photomultiplier acceptance angle for scattered light to 113°. Far-CD measurements (conventional CD) were taken with the photomultiplier 20.5 cm away from the cuvette. Circular differential scattering data are derived from the difference spectra far CD minus near CD and near CD minus fluorscat CD (Figure 1) and are described in full under Results.

Total absorption measurements were made either on a Cary 14 or on a Cary 118; scattering-corrected absorption measurements were done with fluorscat cuvettes as described

above. Fluorscat absorption measurements were corrected for greater than 95% of the total scattering.

Materials. Highly polymerized calf thymus DNA was purchased from Sigma Chemical Co. The DNA was dissolved in phosphate buffer (5 mM phosphate made from 50% monobasic and 50% dibasic sodium phosphate salts and 100 mM NaCl at pH 7.0) to 1–2 mg/mL by stirring slowly overnight at 4 °C. Protein was removed by two extractions with 50:50 chloroform–phenol (distilled and equilibrated with phosphate buffer), followed by a chloroform extraction. The aqueous-layer DNA was precipitated with 2 volumes of 95% ethanol and stored at −20 °C. As needed, the DNA precipitate was pelleted, redissolved, and exhaustively dialyzed against phosphate buffer. The DNA concentration was determined spectrophotometrically and calculated in nucleotides with ϵ_{260nm} = 6600 L/mol·cm (Mahler et al., 1964).

Polylysine with an average degree of polymerization (DP) of 66 and poly(lysine-alanine) (1:1), DP = 260, were obtained as the hydrobromide salts from Sigma Chemical Co. Stock solutions were prepared by dissolving 40–100 mg of polypeptide in 10 mL of phosphate buffer and dialyzing exhaustively against phosphate buffer for subsequent storage at 4 °C with a drop of chloroform. Polypeptide concentrations were determined by nitrogen analysis (Kejdahl determination) and are reported in lysine concentration.

Proflavin hydrochloride was purchased from K & K Laboratories Inc., and ethidium bromide was purchased from Calbiochem-Behring Corp. Hoechst 33342 came from Pharmacia P-L Biochemicals, and the unsubstituted *meso*-tetrakis(4-*N*-methylpyridyl)porphine (H_2TMpyP-4) was purchased as the tosylate salt from Porphyrin Products Inc. The copper(II), nickel(II), and manganese(III) derivatives of H_2TMpyP-4 were a generous gift from R. F. Pasternack [prepared as described by Pasternack et al. (1983a)] and also bought from Porphyrin Products Inc. Standard dye solutions were stored in phosphate buffer at 0.1–1.0 mM dye. Dye concentrations were determined spectrophotometrically with ϵ_{480nm} = 5600 L/mol·cm for ethidium (Waring, 1965), ϵ_{443nm} = 40 400 L/mol·cm for proflavin (Blake & Peacocke, 1966), $\epsilon_{424nm} = 2.26 \times 10^5$ L/mol·cm for H_2TMpyP-4, $\epsilon_{424nm} = 2.31 \times 10^5$ L/mol·cm for Cu^{II}TMpyP-4, $\epsilon_{418nm} = 1.49 \times 10^5$ L/mol·cm for Ni^{II} TMpyP-4, $\epsilon_{463nm} = 0.92 \times 10^5$ L/mol·cm for Mn^{III}TMpyP-4 (Pasternack et al., 1983a), and ϵ_{338nm} = 33 000 L/mol·cm for Hoechst 33342 (in phosphate buffer).

Cellulose dialysis tubing was prepared by boiling in $NaHCO_3$, ethylenediaminetetraacetic acid (EDTA), and sodium dodecyl sulfate, followed by distilled water, and finally phosphate buffer. The dialysis tubing was stored in phosphate buffer with 0.1% NaN_3 at 4 °C and rinsed with distilled water before use.

All other chemicals used were reagent-grade and were used without further purification. Solutions were prepared with distilled water. All experiments, except the preparation of the ψ condensates, were carried out at room temperature.

Preparation of ψ Condensates. Positive ψ condensates were prepared from poly(lysine-alanine) with DNA at an initial nucleotide concentration of 5.0×10^{-5} M and a lysine:phosphate ratio of 0.75. Negative ψ condensates were prepared from polylysine with DNA at an initial nucleotide concentration of 1.0×10^{-4} M and a lysine:phosphate ratio of 0.75. The maximum CD signal from ψ condensates is obtained at a lysine:phosphate ratio of 0.75 for poly(lysine-alanine)(data not shown) and for polylysine (Carroll, 1972). DNA–polypeptide solutions in the appropriate concentrations were prepared at 1.5 M NaCl–5 mM phosphate, pH 7.0 (order of mixing was stock 5 M NaCl in 5 mM phosphate, 5 mM phosphate, at pH 7.0, stock DNA, and stock polypeptide), and subsequently dialyzed to approximately 0.4 M NaCl–5 mM phosphate over the course of 6 h (Carroll, 1972). The ψ condensates were then dialyzed overnight against the standard phosphate buffer to 100 mM NaCl. ψ condensates were used within 48 h of preparation to minimize the loss of ψ-type CD signal caused by aggregation. We observed a loss of up to 10% of the CD amplitude over 48 h. Final concentrations of ψ condensates were determined in nucleotides by fluorscat absorption with ϵ_{260nm} = 6600 L/mol·cm.

Equilibrium Dialysis. Concentrations of dye bound to uncondensed DNA were determined by standard equilibrium dialysis (Cantor & Schimmel, 1980). Equilibrium was 99% complete after 48 h of slow agitation at room temperature. Dye concentrations were determined on both sides of the dialysis cell, since 20–25% of the dye adhered to the membrane. The dye concentration was determined in the DNA-containing side by dissociation of the dye with sodium dodecyl sulfate (SDS)(Pasternack et al., 1983a) at a final concentration of 32 mM SDS. The total absorption was measured on both sides of the dialysis membrane by simple absorption measurements on a Cary 15. In this way, the total concentration of dye bound to the DNA could be determined by subtracting the concentration of dye on the buffer side from the concentration of dye on the DNA-containing side. The extinction coefficients for the dyes in 32 mM SDS are ϵ_{570nm} = 5600 L/mol·cm for ethidium, ϵ_{455nm} = 48 400 L/mol·cm for proflavin, $\epsilon_{426nm} = 2.39 \times 10^5$ L/mol·cm for H_2TMpyP-4, $\epsilon_{429nm} = 2.13 \times 10^5$ L/mol·cm for Cu^{II}TMpyP-4, $\epsilon_{420nm} = 2.25 \times 10^5$ L/mol·cm for Ni^{II}TMpyP-4, $\epsilon_{464nm} = 0.97 \times 10^5$ L/mol·cm for Mn^{III}TMpyP-4, and ϵ_{352nm} = 33 000 L/mol·cm for Hoechst 33342. The amount of bound dye is reported as $1/r$ = nucleotide/dye bound.

Centrifugation of ψ Condensates. Concentrations of dyes bound to positive and negative ψ condensates were determined by spinning down the ψ condensates and measuring the dye concentration in the supernatant to subtract from the total amount of dye added. Five-milliliter samples of ψ condensates and dye at the concentrations used in the CD measurements were spun at 225000*g* for 60 min in a Beckman L2 ultracentrifuge (SW 50L rotor).

Total absorbance measurements on the supernatants showed no remaining scattering components at 320 nm for either the positive or the negative ψ condensates (no dye added). The total absorption of those supernatants at 260 nm showed 98% of the DNA in the positive ψ condensate solution was pelleted and greater than 93% of the DNA in the negative ψ condensate solution was pelleted. Concentrations of dye in the supernatants were determined on a Cary 15 with the extinction coefficients given under Materials.

Results

The apparent CD (conventional CD) of a nucleic acid solution is usually attributed to circular differential absorbance. Total scattering seen in total absorption measurements is assumed to have no effect on CD measurements. For these assumptions, the circular differential extinction ($\epsilon_L - \epsilon_R$) is equal to the circular differential absorption extinction ($a_L - a_R$) in the Beer–Lambert law:

$$\text{apparent CD} = cl(\epsilon_L - \epsilon_R) = cl(a_L - a_R)$$

where c is the concentration and l is the path length. For this case, CD is independent of photomultiplier acceptance angle, and all CD measurements taken along the transmitted beam are equivalent:

far CD (or apparent CD) = near CD = fluorscat CD

In the case of ψ condensates, the apparent CD may have a contribution of greater than 50% from circular differential scattering. This conservative circular differential scattering pattern is as characteristic of the ψ condensate as is the large positive or negative circular differential absorption. To account for this additional circular differential scattering component in the apparent CD, a circular differential scattering contribution ($s_L - s_R$) is added to the circular differential absorption to make up the circular differential extinction:

$$\epsilon_L - \epsilon_R = (a_L - a_R) + (s_L - s_R)$$

The apparent CD as a function of the intensity (I) measured in the CD spectropolarimeter along the transmitted beam is then (Bustamente et al., 1983)

$$\text{apparent CD} = \frac{2}{2.303}\frac{I_R - I_L}{I_R + I_L} = (\epsilon_L - \epsilon_R)cl + \frac{2}{2.303}\frac{\sigma_R(0) - \sigma_L(0)}{2r^2 + \sigma_L(0) + \sigma_R(0)}$$

The second term depends on the distance from the detector to the sample (r) and the molecular circular differential scattering cross-section terms of the sample at 0° [$\sigma_{R,L}(0)$]. The distance r from the detector to the sample is large compared to the molecular circular differential scattering cross-sections, so $1/r^2$ is small. In our measurements, the second term was assumed to be negligible. Figure 1 shows how the experimental CD methods were used to obtain and separate circular differential scattering and circular differential absorption components of the ψ condensates. The fluorscat CD corrects for most of the scattering, leaving only the back-scattering unaccounted for. In order to determine the scattering in the back direction, fluorescence-detected circular dichroism measurements in the back direction with appropriate filters are possible with certain samples (Maestre, 1984). The circular differential scattering data are discussed in terms of two difference spectra for two different scattering cones: the forward scattering cone (from far-CD − near-CD scattering difference spectra) and the side scattering cone (from near-CD − fluorscat CD scattering difference spectra). These two kinds of scattering data reflect the magnitude and sign of the circular differential scattering of the ψ condensate as a function of the scattering angle and allow us to estimate the circular differential scattering envelopes of negative ψ condensates as compared to those of positive ψ condensates (discussed under Circular Differential Scattering of ψ Condensates).

Circular Differential Absorption of Dyes Bound to DNA and ψ Condensates. The dyes studied represent several different types, having a wide variety of CD spectra when bound to DNA. None of the dyes has an intrinsic CD, and none has an induced CD from interaction with polylysine or poly(lysine-alanine). The CD signals in the chromophore regions of the spectra are due to the asymmetry induced by binding to DNA. Figure 2 shows the extrinsic CD of each dye bound to DNA. There are positive, negative, conservative, nonconservative, and more complex CD signals due to the unique interaction of each dye with the DNA bases. There is no simple correlation of pattern or strength between the conservative CD spectra of DNA and the induced CD dye bands resulting from dye binding to the DNA.

Our results show that the circular differential absorbance and circular differential scattering from the dyes bound to the ψ condensates reflect the UV circular differential absorbance and UV circular differential scattering of the ψ condensates

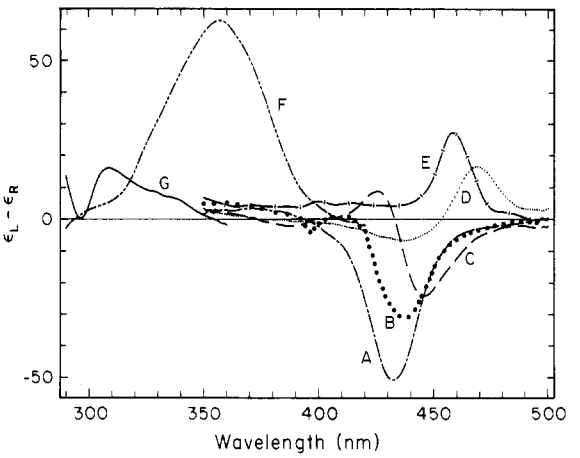

FIGURE 2: CD spectra of dyes bound to uncondensed DNA. The extinction coefficient is in L/cm·M. The ratio of phosphates to bound dye is given as $1/r$. The spectra shown are for the dyes: $Ni^{II}TMpyP$-4, $1/r$ = 17 (A); $Cu^{II}TMpyP$-4, $1/r$ = 18 (B); H_2TMpyP-4, $1/r$ = 17 (C); proflavin, $1/r$ = 15 (D); $Mn^{III}TMpyP$-4, $1/r$ = 21 (E); Hoechst 33342, $1/r$ = 17 (F); ethidium, $1/r$ = 16 (G).

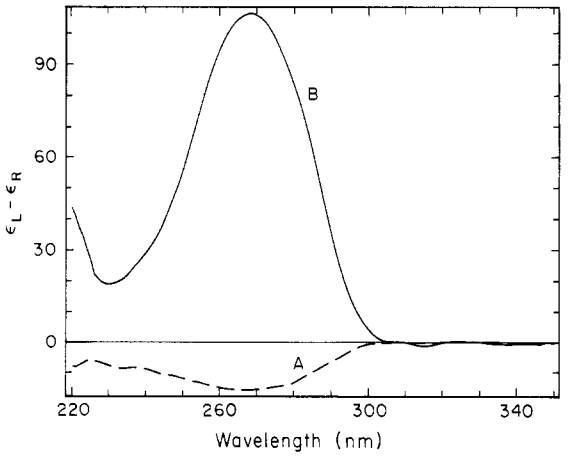

FIGURE 3: Scattering-corrected CD spectra (fluorscat CD) of negative (A) and positive (B) ψ condensates.

with or without dye bound. The UV CD signals of the ψ condensates are not significantly altered on dye binding at low $1/r$ values for those dyes whose CD spectra do not overlap those of DNA. The ψ condensates are formed with DNA as either negative (with polylysine) or positive [with poly(lysine-alanine)]. The UV CD signals of these positive and negative ψ condensates are mimicked in the visible spectrum when intercalative dyes are bound to them. The Hoechst 33342 dye, which binds in the DNA minor groove, shows an inverted CD signal in the dye band (λ_{max} = 360 nm) when compared to the UV CD signal of the ψ condensate, whether positive or negative in magnitude. The other groove-binding dye, $Mn^{III}TMpyP$-4 (Dabrowiak, 1986), shows no detectable visible CD spectrum on binding to either type of ψ condensate.

Figure 3 shows the large characteristic scattering-corrected CD spectra (fluorscat CD) of positive and negative ψ condensates without dye bound. Figure 4 shows the visible scattering-corrected CD spectra for all of the dyes bound to negative ψ condensates, and Figure 5 shows the visible fluorscat or near scattering-corrected CD spectra of the dyes with the positive ψ condensates. For fluorescent dyes, near-CD measurements with large photomultiplier acceptance angles were used. For all other dyes, fluorscat CD measurements were used. For example, $Cu^{II}TMpyP$-4 has a negative scattering-corrected CD when bound to negative ψ condensates (spectrum B, Figure 4) and a positive scattering-corrected CD when

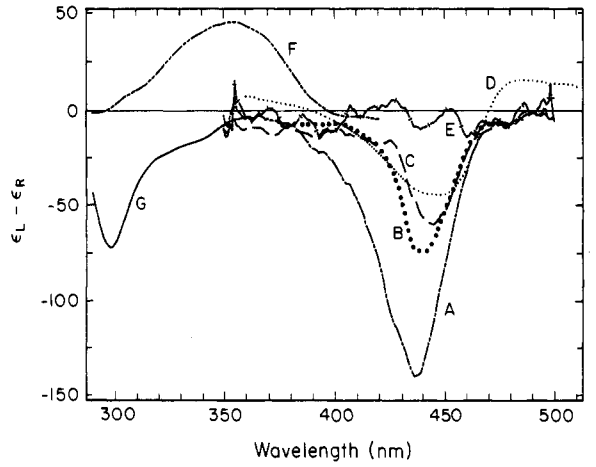

FIGURE 4: Scattering-corrected CD spectra (fluorscat and near CD) of dyes bound to negative ψ condensates. The spectra shown are for the dyes: $Ni^{II}TMpyP-4$, $1/r = 25$ (A); $Cu^{II}TMpyP-4$, $1/r = 20$ (B); $H_2TMpyP-4$, $1/r = 24$ (C); proflavin, $1/r = 34$ (D); $Mn^{III}TMpyP-4$, $1/r = 57$ (E); Hoechst 33342, $1/r = 19$ (F); ethidium, $1/r = 20$ (G). We took fluorscat CD spectra for the porphyrins. Due to fluorescence, near CD was the closest possible approximation to circular differential absorption for ethidium, proflavin, and Hoechst 33342.

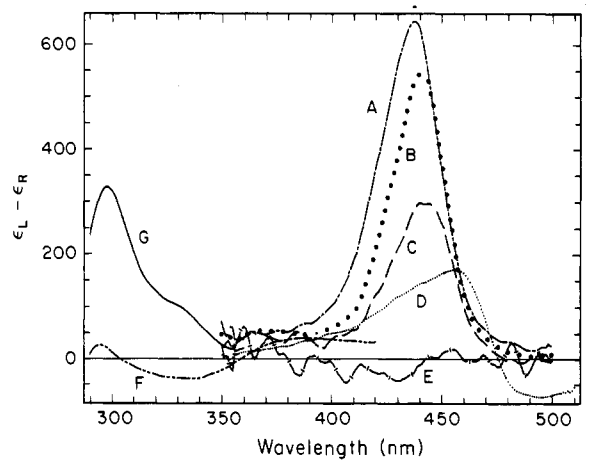

FIGURE 5: Scattering-corrected CD spectra (fluorscat and near CD) of dyes bound to positive ψ condensates. The spectra shown are for the dyes: $Ni^{II}TMpyP-4$, $1/r = 30$ (A); $Cu^{II}TMpyP-4$, $1/r = 34$ (B); $H_2TMpyP-4$, $1/r = 42$ (C); proflavin, $1/r = 48$ (D); $Mn^{III}TMpyP-4$, $1/r = 94$ (E); Hoechst 33342, $1/r = 19$ (F); ethidium, $1/r = 19$ (G). We took fluorscat CD spectra for the porphyrins. Due to fluorescence, near CD was the closest possible approximation to circular differential absorption for ethidium, proflavin, and Hoechst 33342.

bound to positive ψ condensates (spectrum B, Figure 5). In general, the dye CD signals in Figure 4 as compared to Figure 5 are approximately inverted, just as the scattering-corrected CD signals in Figure 3 are inverted for the positive ψ condensates vs. the negative ψ condensates without dye bound. As explained at the beginning of this section and shown in Figure 1, fluorscat CD and near CD partially correct for scattering and are used as approximations to the true circular differential absorption.

The sign of the dye-induced scattering-corrected CD can be experimentally related to the mode of dye binding. Ethidium (LePecq & Paoletti, 1967), proflavin (Armstrong, 1969), $H_2TMpyP-4$, $Cu^{II}TMpyP-4$, and $Ni^{II}TMpyP-4$ (Pasternack et al., 1984) are intercalators and occupy sites similar to those of the DNA bases. As a result, the induced circular differential scattering and circular differential absorption spectra of these dyes bound to ψ condensates mimic the UV spectra of the ψ condensates. Both the shape and magnitude of the scattering-corrected CD dye band reflect the

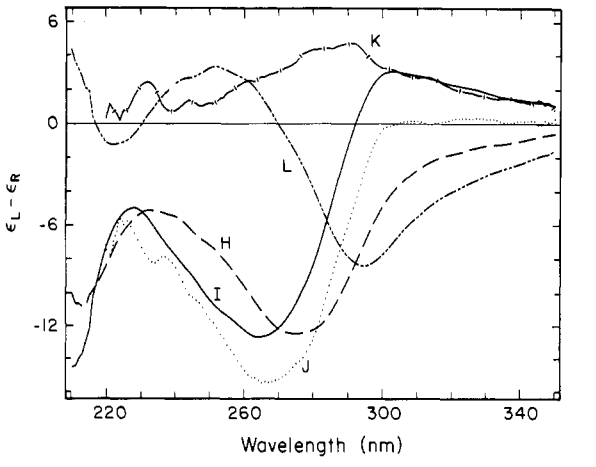

FIGURE 6: Circular differential scattering and scattering-corrected CD spectra for negative ψ condensates. The spectra and difference spectra shown are far CD (H), near CD (I), fluorscat CD (J), side scattering (K), and forward scattering (L).

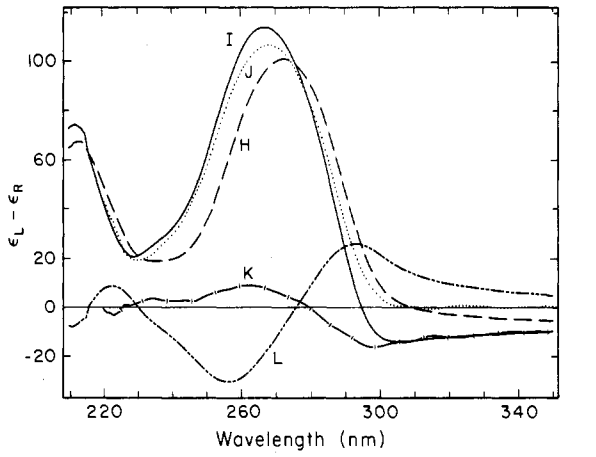

FIGURE 7: Circular differential scattering and scattering-corrected CD spectra for positive ψ condensates. The spectra and difference spectra shown are far CD (H), near CD (I), fluorscat CD (J), side scattering (K), and forward scattering (L).

shape and strength of the scattering-corrected CD band of the positive or negative ψ condensates in the UV. Interpretation of the bound ethidium spectra (spectra G, Figures 4 and 5) is somewhat complex due to significant energy exchange that may occur between the condensed DNA (scattering-corrected CD $\lambda_{max} = 265$ nm) and the ethidium (scattering-corrected CD $\lambda_{max} = 305$ nm). Even so, the scattering-corrected CD of ethidium bound to ψ condensates does essentially mimic the scattering-corrected CD of the of the ψ condensates, as expected for an intercalator. The two nonintercalating dyes studied, $Mn^{III}TMpyP-4$ and Hoechst 33342, do not show ψ spectra mimicking CD patterns when bound to ψ condensates. Both of these dyes bind with their average transition dipole moments out of the DNA base plane. However, the orientation of the Hoechst dye gives an inversion of the ψ condensate circular differential absorption and scattering.

Circular Differential Scattering of ψ Condensates. In addition to a characteristic large circular differential absorption band, ψ condensates have characteristic conservative circular differential scattering patterns centered around the circular differential absorption band (Figures 6 and 7). Circular differential scattering measurements are a function of acceptance angle. We divide the scattering space around the ψ condensate (a function of angle) in four sections: forward scattering (far CD − near CD), side scattering (near CD −

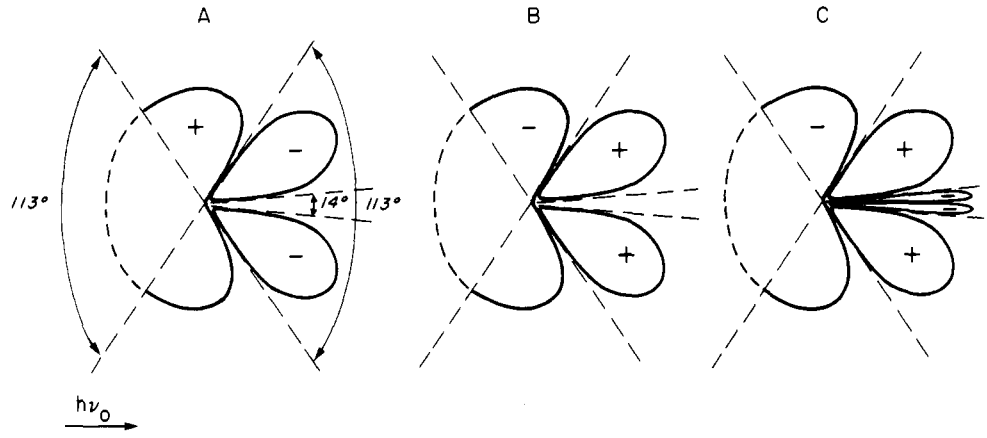

FIGURE 8: Scattering envelope patterns for positive ψ condensates. From the two circular differential scattering difference spectra, the scattering envelope at lower wavelengths from the 270-nm scattering-corrected CD band maximum is shown on the left (A). The scattering envelope between 270 and 310 nm is shown in the center (B). The scattering envelope at higher wavelengths from 310 nm is on the right (C).

fluorscat CD), back-scattering (not accounted for in our analysis), and differential scattering at 0° (cannot be separated from circular differential absorption in the far CD measurement) (see Figure 1). The forward scattering difference spectrum of negative ψ condensates (spectrum L, Figure 6) is positive at wavelengths lower (λ < 265 nm) than the scattering-corrected CD (fluorscat CD) minimum and negative at wavelengths higher (λ > 265 nm) than the scattering-corrected CD minimum. In the case of positive ψ condensates, the forward scattering difference spectrum is also conservative about the scattering-corrected CD but is inverted in sign (spectrum L, Figure 7). The side scattering difference spectrum of the positive ψ condensates (spectrum K, Figure 7) is the inverse of the forward scattering spectrum (spectrum L). This is also seen with the negative ψ condensates (spectrum K, Figure 6), but there appears to be a base-line shift due to far-UV scattering. These circular differential scattering data allow a simple sketch of the circular differential scattering envelope of a positive ψ condensate (Figure 8). The scattering lobes are drawn by examining the forward scattering difference spectrum and the side scattering section. A positive lobe in a particular direction means that the particle scatters more left circularly polarized light than right circularly polarized light in that direction. In the positive ψ condensate scattering envelope, in the 270–310-nm range (B, Figure 8), the positive lobe dominates in the forward scattering difference spectrum (spectrum L, Figure 7), whereas the negative lobe dominates in the side scattering difference spectrum (spectrum K, Figure 7). At wavelengths greater than 310 nm, the far-CD spectrum of the positive ψ condensate has a significant negative tail (spectrum H, Figure 7), which must be due to circular differential scattering in the true forward direction (close to 0°), since the scattering is corrected only by fluorscat and there are no chromophores in that region of the spectrum. To explain this negative tail, the scattering envelope of the positive ψ condensate must then have gained an additional negative set of lobes at higher wavelengths from 310 nm (C, Figure 8). We speculate that this negative circular differential scattering tail arises from a very large contribution from a far-UV scattering pattern of opposite sign. Both the negative and positive ψ condensates have near-CD minus far-CD forward scattering difference spectra from 210 to 230 nm (spectra L, Figures 6 and 7), which suggest this kind of opposite sign scattering pattern in the far UV. The negative ψ condensate scattering envelope (not shown) is similar to that of the positive ψ condensate, but the lobes have opposite signs, and the additional set of lobes that appear at greater than 310 nm in the positive ψ condensate are not present in the negative ψ condensate.

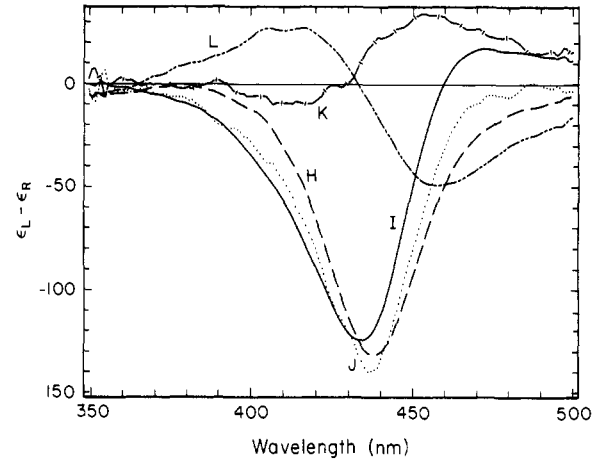

FIGURE 9: Circular differential scattering and scattering-corrected CD spectra for Ni^{II}TMpyP-4 bound to negative ψ condensates at $1/r$ = 25. The spectra and difference spectra shown are far CD (H), near CD (I), fluorscat CD (J), side scattering (K), and forward scattering (L). These measurements have the corresponding negative ψ condensate background subtracted.

Circular Differential Scattering of Dyes Bound to ψ Condensates. The long-range chiral packing model of the ψ condensates also explains the induced circular differential scattering of dyes bound to ψ condensates. As with the scattering-corrected CD data, the visible circular differential scattering patterns of a dye intercalated into a ψ condensate mimic the UV circular differential scattering patterns of that ψ condensate. Figure 9 shows all of the dye band circular differential scattering and CD absorption data for Ni^{II}TMpyP-4 bound to negative ψ condensates. The general shapes and patterns of the spectra are the same as the corresponding UV CD spectra for the negative ψ condensates to which the Ni^{II}TMpyP-4 is bound (Figure 6). For example, the forward scattering difference spectrum (labeled L) in both the induced Ni^{II}TMpyP-4 band and the UV negative ψ band is positive at higher wavelengths from the scattering-corrected CD minimum and negative at lower wavelengths from the scattering-corrected CD minimum. In addition, these forward scattering difference spectra are approximately half the magnitude (from the origin to the minimum or maximum signal) of the fluorscat CD signals (spectra J). A long-range chirally packed structure is consistent with these data. The four other intercalative dyes also show this mimicking of the

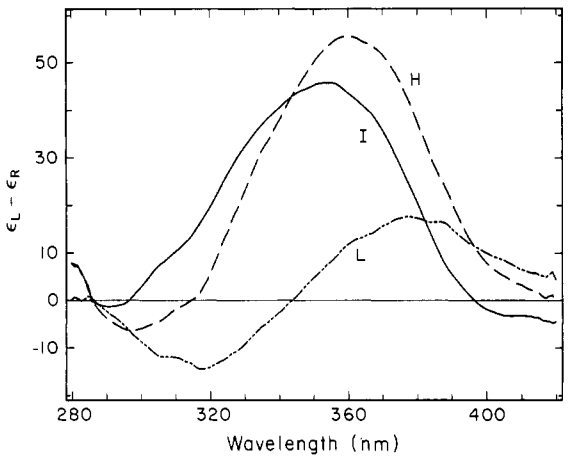

FIGURE 10: Circular differential scattering and scattering-corrected CD spectra for Hoechst 33342 bound to negative ψ condensates at $1/r = 19$. The spectra and difference spectra shown are far CD (H), near CD (I), and forward scattering (L). These measurements have the corresponding negative ψ condensate background subtracted.

CD scattering pattern (data not shown). The CD data for the Hoechst 33342 bound to *negative* ψ condensates are shown in Figure 10. Just as the scattering-corrected CD (near CD is the closest approximation for this fluorescent dye, labeled I in Figure 10) is *positive* for this dye bound to negative ψ condensates, the forward scattering difference spectrum (spectrum L) is the inverse of that seen for the negative ψ condensates (spectrum L, Figure 6). As with the scattering-corrected CD results for Mn^{III}TMpyP-4, forward and side scattering signals are also on the order of the Cary 60 noise, suggesting the Mn^{III}TMpyP-4 is binding with its transition dipole moment along the DNA long axis. We are unable to eliminate the possibility that the Mn^{III}TMpyP-4 is binding randomly to the ψ condensates, resulting in no ψ-type CD's.

Binding Studies. Equilibrium dialysis results on the binding of the dyes to calf thymus DNA at the ratios of dye to phosphate used in the CD experiments showed Ni^{II}TMpyP-4, Cu^{II}TMpyP-4, and H_2TMpyP-4 were greater than 95% bound, Mn^{III}TMpyP-4 was 80% bound, Hoechst 33342 was 88% bound, proflavin was 73% bound, and ethidium was greater than 53% bound.

The binding of the dyes to negative ψ condensates was not as strong as that to uncondensed DNA, and the binding of the dyes to positive ψ condensates was even weaker. The ultracentrifuge experiments gave the percentage of dye bound to negative ψ condensates under our CD conditions as follows: Ni^{II}TMpyP-4, 67%; Cu^{II}TMpyP-4, 85%; H_2TMpyP-4, 71%; Mn^{III}TMpyP-4, 30%; proflavin, 35%; ethidium, 44%; Hoechst 33342, 94%. The percentage of dye bound to positive ψ condensates was as follows: Ni^{II}TMpyP-4, 54%; Cu^{II}TMpyP-4, 52%; H_2TMpyP-4, 43%; Mn^{III}TMpyP-4, 18%; proflavin, 22%; ethidium, 42%; Hoechst 33342, 90%.

To investigate the binding complexity of the dyes, we examined the binding of Ni^{II}TMpyP-4 as a representative dye, to uncondensed calf thymus DNA, and to negative ψ condensates at different binding ratios (from $1/r = 12$ to $1/r = 47$). The Ni^{II}TMpyP-4 was completely bound to uncondensed DNA at $1/r = 16$ and higher and 96% bound at $1/r = 12$. Compared to the uncondensed DNA binding, Ni^{II}TMpyP-4 binding to negative ψ condensates had a much lower equilibrium constant. Over the binding ratios used, the Ni^{II}TMpyP-4 was bound 57% ($1/r$ low) to 88% ($1/r$ high). A Scatchard plot of Ni^{II}TMpyP-4 bound to negative ψ condensates was a smooth concave down curve (data not shown), implying cooperativity in binding to the condensed DNA. Therefore, the extinction coefficients of the dyes bound to condensed DNA are a function of the ratio $1/r$. The study on Ni^{II}TMpyP-4 binding to ψ condensates showed a maximum CD extinction coefficient at $1/r = 27$. Below $1/r = 27$, there is probably some destruction of the ψ condensate, and at $1/r > 27$ the resonance phenomenon decreases as the dye molecules get too far apart to report the long-range periodicity of the ψ condensate.

To show that these results are general, we repeated most of the measurements with positive and negative ψ condensates made with double-stranded poly(dG-dC) and poly(dA-dT). These condensates have even larger circular differential scattering and circular differential absorption components and show similar predictable patterns when bound with dyes.

Discussion

ψ condensates have some of the largest CD coefficients known. Similarly, the dyes that have specific binding sites on dispersed DNA (intercalators or groove binders) have extremely large CD coefficients when bound to ψ condensates. In addition to having large, easy to detect signals, dyes bound to ψ condensates show circular differential scattering and scattering-corrected CD patterns that reflect the type of ψ condensate (positive or negative) to which the dyes are bound. We consider here first the anomalous ψ-type signals, second the manifestation of those signals in the induced dye band when dyes are bound to ψ condensates, and third the implications of these results.

ψ-Type Signal. Our results show ψ condensates have anomalous scattering-corrected CD and circular differential scattering signals because of the long-range chiral structure of the DNA. Our interpretation of the CD behavior of the ψ condensates bound with dyes is related to recent theoretical models proposed by Keller et al. (1985; on circular differential scattering) and Kim et al. (1986; on circular differential absorption). The theoretical treatment of Keller et al. successfully predicts the circular differential scattering from a microscopic helix and from the stacked chiral array found in cholesteric liquid crystals. The calculations are based on a finite number of polarizable groups possessing only one electronic transition between 200 and 320 nm. Kim et al. similarly predict ψ-type circular differential absorption signals resulting from three-dimensional, dense, chirally arranged point polarizable groups. Although a ψ condensate is considerably more complex than a simple set of point-polarizable groups, much of the theory appears to account for the spectroscopic phenomena we see.

We interpret the mimicking pattern seen in the dye band of intercalators bound to the ψ condensates as a resonance phenomenon of aligned transition dipole moments (Kim et al., 1986). Proflavin, ethidium, H_2TMPyP-4, Ni^{II}TMpyP-4, and Cu^{II}TMpyP-4 have transition dipole moments in approximately the same set of planes as those of the DNA bases and are expected to occupy similar sites in any long-range interaction as the bases themselves. We believe the ψ condensates have long-range structural periodic repeats within an order of magnitude of the wavelength of UV or visible light (Kim et al., 1986). When the large chiral repeat structure interacts with the chiral light, it behaves as an antenna, and there is a resonance phenomenon at the induced dye band resulting in the large circular differential absorption and circular differential scattering. The resonance phenomenon is thought to arise in the visible due to electronic coupling of the dyes over a long range and is not due solely to nearest-neighbor or next-to-nearest-neighbor effects. Figure 11 is a possible model of a ψ condensate [similar to a model proposed by Schellman

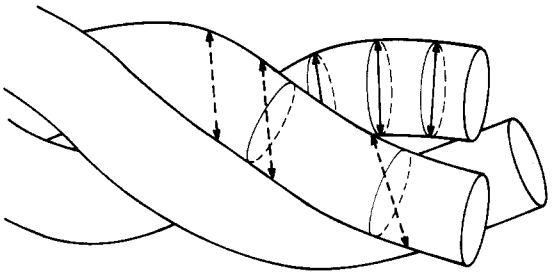

FIGURE 11: Hypothetical model of a ψ condensate with bound dyes. Many of the strands of these DNA and polylysine or poly(lysine-alanine) groups may be closely packed in a chiral arrangement such as a helix. Planar intercalators are bound with their planes in the same set of planes as the DNA bases (line arrows represent intercalator planes). Minor groove binding dyes are bound with their long axis or average transition dipole moment at an angle out of the DNA base planes, aligned in the DNA minor groove (dashed arrows represent dipoles of minor groove binding dyes).

and Parthasarathy (1984) for DNA condensed with polyamines] to which intercalative dyes are bound at sites similar to those the DNA bases occupy.

The CD spectra of the two nonintercalating dyes, Hoechst 33342 and Mn^{III}TMpyP-4, when bound to ψ condensates can also be explained in terms of a long-range chiral structure. When Hoechst 33342 binds in the minor groove of the ψ DNA, it has an average transition dipole well out of the plane of the DNA base pairs, so it is not expected to have a CD signal like that of the bases or intercalators. However, the Hoechst 33342 is still binding at specific sites on the DNA in the long-range chirally ordered ψ condensate, and the CD signals of the bound dye should reflect that long-range chiral order. The bound Hoechst 33342 does report that long-range chiral structure and has CD spectra inverted to those observed for intercalative dyes. Figure 11 shows how a minor groove specific dye that binds uniformly could report the long-range chiral structure of a ψ condensate. We propose two possible explanations for why the Mn^{II}TMpyP-4 has negligible CD when bound to ψ condensates. Although the dye has been shown to bind in the minor groove of DNA at the ratios we used, (Dabrowiak, 1986), it may bind nonuniformly within the minor groove, with respect to the DNA bases, such that it cannot report a long-range chiral repeat unit. This is equivalent to saying the effective polarizability tensor in the model of Kim et al. (1986) is spherical. Mn^{II}TMpyP-4 may in fact have a specific orientation with respect to the DNA bases, but the orientation may simply give very small circular differential absorption and circular differential scattering. If there are dye orientations with respect to the DNA bases in the ψ condensates that give mimicking CD spectra (such as those of intercaltors) and there are dye orientations that result in inverted ψ-type spectra in the dye band, it follows that there may be dye orientations where there is no reporting of the ψ-type signal in the dye band.

Most researchers agree that the ψ-type CD signals seen in many kinds of DNA condensates are due to long-range chiral order, not simply secondary DNA structure. The secondary structure of the DNA probably changes very little upon condensation. X-ray scattering of DNA condensed with poly(ethylene oxide) and NaCl (Maniatis et al., 1974) showed that the ψ condensate had approximately the B-form secondary structure that it ordinarily has when dispersed in solution. However, Maniatis et al. (1974) did not find any evidence for supercoiling. This probably indicates the long-range chiral order was not regular enough to be seen in X-ray scattering measurements. Most of the disagreement on DNA condensates is in proposing the actual structure of the long-range chiral order that gives rise to the ψ-type CD. Since there are many different preparations of condensed DNA that give ψ-type CD's, it is reasonable that there may be several kinds of long-range chiral order. Electron microscopy on sppermidine–DNA condensates (Marx & Ruben, 1983) showed that these particular condensates are toroids. On the other hand, Kielland and Williams (1976) used electron microscopy to observe negative ψ condensates formed from DNA and poly(amino acids) by NaCl gradients and found many different preparation-dependent condensates. Using X-ray diffraction to address the structure within polyamine–DNA condensates, Schellman and Parthasarathy (1984) discard the notion of stabilization due to long-range electrostatic repulsive and attractive forces but suggest the condensate is some sort of liquid crystal with counterions between the helices resulting in a stable three-dimensional phase of high structural order. This liquid-crystalline state is also the model favored by Kielland and Williams (1976). DNA condensates may have enough long-range order to show that order in X-ray diffraction studies (Maniatis et al., 1974; Schellman & Parthasarathy, 1984), but there may be enough long-range chiral order to affect the CD of the DNA condensates. Our results are consistent with a ψ condensate model in which there are many small liquid-crystal-like structures (see Figure 11), aggregated with sufficient long-range chiral order to have anomalous CD.

Evdokimov et al. (1983) have also done some experiments that may be discussed in terms of how the alignment and long-range coupling of the dye transition dipole moments with those of the DNA bases give the special induced CD signals in dyes bound to ψ condensates. They condensed DNA with daunomycin and poly(ethylene glycol) to get a full range of positive and negative ψ condensates. The intercalating daunomycin behaved as a reporter molecule in the visible region of the spectrum and followed a similar CD pattern in the visible as was occurring in the UV. Dissociation of the ψ condensates with SDS did not significantly change the CD of the particles, so the reversal in sign of the optical activity between positive and negative ψ condensates was attributed to major differences in the long-range chiral order, rather than local differences due to the presence of the dye.

Applications. Using information on how the transition dipole moments of the bound dyes are aligned with those of the DNA bases, it may be possible to distinguish between different types of dye binding by comparing the visible CD signals of dyes bound to ψ condensates with the UV CD signals of the ψ condensates. At the present, distinguishing between groove-binding dyes, intercalators, and nonspecific dyes typically involves temperature jump experiments (Pasternack et al., 1983b) or DNA restriction fragment footprinting (in the case of some groove binders; Harshman & Dervan, 1985) or X-ray diffraction (which is conclusive, but requires crystals). With an estimate of the direction of a dye transition dipole moment, binding a dye of unknown specificity to positive and negative ψ condensates gives information on dye binding orientation. A dye that followed the CD mimicking patterns of an intercalator or the inverse CD patterns of a groove binder when bound to both positive and negative ψ condensates would likely be an intercalator or groove binder, respectively.

CD Anomalies in Other Systems. CD anomalies besides ψ condensates have also been studied. Some of the dyes may be useful as reporter molecules for studying non nucleic acid systems, where there is long-range chiral order. Acridine orange has been used in glycosaminoglycans as both the aggregator and the reporter molecule, in work similar to that of Evdokimov et al. on DNA condensates (Salter et al., 1976).

The visible CD band of the acridine orange bound to the glycosaminoglycans also mimicked the connective tissue UV CD band.

CD studies on Chinese hamster ovary cells (Maestre et al., 1985) are an example of a complex system where scattering-corrected CD and circular differential scattering give complementary information. In this case, they were used together to study the chromatin signal as an indicator of the cell cycle phase. Dyes bound to such complex systems could be of use in selectively examining components of the UV CD spectrum and in understanding more about the structure to which the dyes are bound (in this case chromatin). Dyes that specifically bind DNA, such as Hoechst dyes, some of which are fluorescent when bound to DNA but not RNA (Cesarone et al., 1979), may be used to study the long-range chiral order of complex systems of proteins and nucleic acids by isolating specific signals in the visible region of the spectrum. This isolation of signals from one part of a structure might also allow for kinetic studies. The recently developed differential polarization light microscope (Mickols et al., 1985) is one place where the dyes could be used on complex systems. Dyes may also be used to distinguish between nucleic acid order in one system and nucleic acid order in another, provided the ordered structures being examined had unique scattering-corrected CD and circular differential scattering signals. It would be interesting to see how widespread the ψ-type signal is in complex biological systmes, such as whole cells.

One area where this research might be useful is in experimental circular differential intensity scattering (CIDS) measurements. Recently, there has been some theoretical work on the CIDS close to an absorption band (Kim et al., 1986). CIDS experiments on dyes, with absorption maxima in the visible, bound to ψ condensates would provide a good test of the theory.

Acknowledgments

We thank Professor R. F. Pasternack for his generous gift of the porphyrins, and we gratefully acknowledge J. Corbett for donating the first ψ condensates and demonstrating their preparation.

References

Blake, A., & Peacocke, A. R. (1966) *Biopolymers 4*, 1091–1104.

Bustamente, C., Tinoco, I., Jr., & Maestre, M. F. (1983) *Proc. Natl. Acad. Sci. U.S.A. 80*, 3568–3572.

Cantor, C. R., & Schimmel, P. R. (1980) in *Biophysical Chemistry*, Part III, pp 13328–1330, Freeman, San Francisco.

Carroll, D. (1972) *Biochemistry 11*, 421–425.

Cesarone, C. F., Bolognesi, C., & Santi, L. (1979) *Anal. Biochem. 100*, 188–197.

Dabrowiak, J. (1986) *Biophys. J. 47*, 3889.

Ellerton, N. F., & Isenberg, I. (1969) *Biopolymers 8*, 767–786.

Evdokimov, Y. M., Salyanov, V. I., Dembo, A. T., & Berg, H. (1983) *Biomed. Biochim. Acta 42*, 855–866.

Gray, D. M., Edmondson, D. P., Lang, D., Vaughn, M. R., & Nave, C. (1979) *Nucleic Acids Res. 6*, 2089–2107.

Harshman, K. D., & Dervan, P. B. (1985) *Nucleic Acids Res. 13*, 4825–4835.

Jordan, C. F., Lerman, L. S., & Venable, J. H., Jr. (1972) *Nature (London), New Biol. 236*, 67–70.

Keller, D., Bustamente, C., Maestre, M. F., & Tinoco, I., Jr. (1985) *Biopolymers 24*, 783–797.

Kielland, S. L., & Williams, R. E. (1976) *Can. J. Chem. 54*, 3884–3894.

Kim, M., Ulibarri, L., Keller, D., Maestre, M. F., & Bustamente, C. (1986) *J. Chem. Phys. 84*(6), 2981–2989.

Kopka, M. L., Yoon, C., Goodsell, D., Pjura, P., & Dickerson, R. E. (1985) *Proc. Natl. Acad. Sci. U.S.A. 82*, 1376–1380.

Lefevre, G. (1976) in *The Genetics and Biology of Drosophila* (Ashburner, M., & Novitske, E., Eds.) pp 23–67, Academic, San Francisco.

LePecq, J. B., & Paoletti, C. (1967) *J. Mol. Biol. 27*, 87–106.

Lerman, L. S. (1973) in *Physico-Chemical Properties of the Nucleic Acids* (Duchesne, J., Ed.) Vol. 3, pp 59–76, Academic, New York.

Lindsley D., & Tokuzasu, K. (1980) *The Genetics and Biology of Drosophila* (Ashburner, A., & Wright, T., Eds.) Vol. 2d, pp 226–294, Academic, San Francisco.

Maestre, M. F. (1984) *Optical Techniques in Biological Research* (Rousseau, D. L., Ed.) Chapter 5, pp 291–341, Academic, New York.

Maestre, M. F., & Reich, C. (1980) *Biochemistry 19*, 5214–5223.

Maestre, M. F., Salzman, G. C., Tobey, R. A., & Bustamente, C. (1985) *Biochemistry 24*, 5152–5157.

Mahler, H. R., Kline, B., & Mehrota, B. D. (1964) *J. Mol. Biol. 9*, 801–811.

Maniatis, T., Venable, J. H., Jr., & Lerman, L. S. (1974) *J. Mol. Biol. 84*, 37–64.

Marx, K. A., & Ruben, G. C. (1983) *Nucleic Acids Res. 11*(6), 1839–1854.

Mickols, W., Maestre, M. F., Tinoco, I., Jr., & Embury, S. H. (1985) *Proc. Natl. Acad. Sci. U.S.A. 82*, 6527–6531.

Müller, W., & Crothers, D. M., (1968) *J. Mol. Biol. 35*, 251–290.

Pasternack, R. F., Gibbs, E. J., & Villafranca, J. J. (1983a) *Biochemistry 22*, 2406–2415.

Pasternack, R. F., Gibbs, E. J., & Villafranca, J. J. (1983b) *Biochemistry 22*, 5409–5417.

Pasternack, R. F., Antebi, A., Ehrlich, B., Sidney, D., Gibbs, E. J., Bassner, S. L., & Depoy, L. M. (1984) *J. Mol. Catal. 23*, 235–242.

Reich, C., Maestre, M. F., Edmondson, S., & Gray, D. M. (1980) *Biochemistry 19*, 5208–5213.

Salter, M. K., Rippon, W. B., & Abrahamson, E. W. (1976a) *Biopolymers 15*, 1213–1227.

Salter, M. K., Rippon, W. B., & Abrahamson, E. W. (1976b) *Biopolymers 15*, 1251–1265.

Schellman, J. A., & Parthasarathy, N. (1984) *J. Mol. Biol. 175*, 313–329.

Schmechel, D. E. V., & Crothers, D. M. (1971) *Biopolymers 10*, 465–480.

Tunis-Schneider, M. J. B., & Maestre, M. F. (1970) *J. Mol. Biol. 52*, 521–541.

Turner, D. H., Tinoco, I., Jr., & Maestre, M. F. (1974) *J. Am. Chem. Soc. 96*, 4340–4342.

Waring, M. J. (1965) *J. Mol. Biol. 13*, 269–282.